

The Impact of Bubble-Bubble Interaction on Anodic Gas Release: A Water Model Analysis

Are J. Simonsen¹, Kristian Etienne Einarrud² and Ingo Eick³

¹ SINTEF Materials and Chemistry, Trondheim, Norway

² HIIST, Trondheim, Norway

³ Hydro Aluminium Deutschland GmbH, Neuss, GERMANY

Keywords: Hall-Héroult cell, Bubble dynamics, surface tension, water model experiments.

Abstract

A water model of the lab scale electrolysis cell presented previously has been constructed to investigate bubble coalescence and movement under a surface with varying inclination. Bubble generation is simulated by passing N₂ gas through a porous ceramic plate representing the anode. Experiments have been performed with three different liquids; tap water, and tap water mixed with ethanol or NaCl, aiming primarily to study the influence of varying surface tension at different anode inclinations and gas flow rates. Gas bubble behavior is tracked using a high speed camera. A strong dependence upon fluid properties is observed when considering the gas flow behavior with respect to bubble size, velocities and flow pattern in general. The results indicate that only the NaCl solution is able to reproduce the self-organized state expected from corresponding electrolysis experiments. Results indicate that this feature is mainly due to different wetting behavior of the different fluids considered.

Introduction

In the Hall-Héroult electrolysis process, gas bubbles play an important role. Gas bubbles, consisting mainly of CO₂, are a by-product of the electrolytic process. Bubbles are generated at the anode and buoyancy drives them to the bath surface. The drag from the drifting bubbles generates a flow that stirs the bath and distributes alumina. In the interpolar region (the ACD), bubbles are considered as the main driving force [1]. Bubbles also have a negative effect on the process due to their negligible electrical conductivity, increasing the voltage drop between the anode and the cathode by about 250 mV [2].

This two-sided influence of the bubbles calls for carefully designed cells that promote the desired flow pattern and minimize the thickness of the bubble layer. Such a design requires a fundamental understanding of the process. However, the number of parameters and physical phenomena involved are large and complex, and the environment is extremely hostile to accurate measurements. In this context small scale physical models of the anode have appeared as an attractive way of studying the underlying physical phenomena. Alam et al. [3] gave a review of the different works performed on small scale models. A major concern in these types of models is how to represent the real phenomena and flow situation realistically in a scaled model. Since bubble flow is the main flow generating mechanism, it appears crucial to obtain similar bubble flow in the model as in the real system. This is a considerable task since the details of the full scale flow, such as bubble size, velocity, bath fluid properties etc., is unknown.

The aim of the current study was to vary surface tension and study the effect this had on the behavior of nitrogen bubbles generated

under an inclined porous plate. Besides surface tension the wetting conditions are modified by the water additives.

Description of experiment

The experimental setup is representing a laboratory cell experiment with polarization for investigating bubble release [4]. Bubble flow simulations have been carried out to describe the self-organized bubble release in the experiment [5], which shall be interpreted now with the water model. A simplified setup for determining the bubble behavior that is more comparable to the real anode bubble flow was chosen. Using a single phase fluid with good transparency made it possible to film from the bottom. This allows us to follow the bubble growth and transport as it flows along the anode surface.

Experimental setup

The cathode is represented with a 23.1cm wide quadratic container made out of 8mm thick Plexiglas (Figure 1). The anode, a porous ceramic plate, was placed in the centre and approximately 2.5cm from the bottom of the box. The box was filled with 3.1 litre of tap water, equal to a 6.1 cm water height above the bottom of the box. Nitrogen gas was injected from the wall outlet, through a rubber hose via a flow meter, and then pushed through the porous ceramic plate. Below the box a 22W ring light was positioned about 16cm below the box. The camera, SANYO Xacti VPC-HD2000, was placed at a distance of about 30cm from the bottom of the box. Gas and water temperature was read manually and logged for each sample during the experiment. Figure 1 gives an overview of the box and anode dimensions.

In each experiment the anode was inclined in the lateral direction with accuracy within 0.1° and a recording of minimum 60s was taken. After recording all positions, the first recorded position was retaken and compared to the first recording of the set in order to identify possible changes in the system.

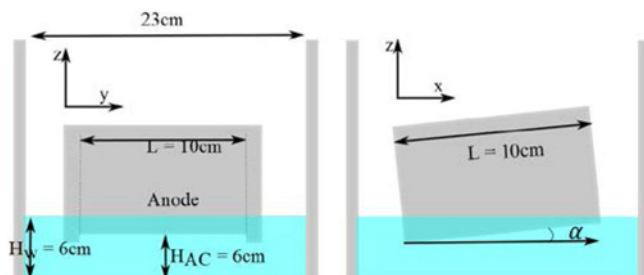


Figure 1: Anode size and box dimensions of used in water model experiments.

Fluid properties

Fluids were selected with the aim of varying the surface tension, with tap water as a reference. For reduction of surface tension ethanol was added in different concentrations. As seen in Table 1 adding 10% in weight of ethanol reduces the surface tension by 34% at $T = 20^\circ\text{C}$. The viscosity of the tap water-ethanol mixture was calculated after the three step procedure outlined in [6].

| $T = 20^\circ\text{C}$ | wt % | X | $\sigma [\text{mN/m}]$ | $\delta\sigma [\%]$ | $\rho [\text{kg/m}^3]$ | $\nu [\text{cSt}]$ | $\mu [\text{mPas}]$ |
|------------------------|------|-------|------------------------|---------------------|------------------------|--------------------|---------------------|
| Exp. | 0 | 0.0 % | 72.8 | 0 % | 998.2 | 1.004 | 1.002 |
| | 5 % | 2.0 % | 56.4 | -22 % | 985.3 | 1.023 | 1.008 |
| | 10 % | 4.2 % | 48.1 | -34 % | 972.6 | 1.043 | 1.014 |
| | 15 % | 6.5 % | 42.7 | -41 % | 960.4 | 1.063 | 1.021 |
| | 20 % | 8.9 % | 38.6 | -47 % | 948.4 | 1.084 | 1.028 |

Table 1: Surface tension and density of water-ethanol mixtures at 20°C [7].

Water density and viscosity were only slightly modified by about 3% at 10% ethanol addition.

To increase the surface tension, table salt, mainly NaCl, was added. Salt has much less impact per weight percentage than ethanol, and solubility sets a limit on how much can be added. Table 2 shows experimental and extrapolated values for some essential mixture properties when the weight percentage of salt is varied. Viscosity and density of the mixture was found by linear inter-/extrapolation from the experimental data found in [8] [9].

| $T = 20^\circ\text{C}$ | wt % | X | $\sigma [\text{mN/m}]$ | $\delta\sigma [\%]$ | $\rho [\text{kg/m}^3]$ | $\nu [\text{cSt}]$ | $\mu [\text{mPas}]$ |
|------------------------|------|-------|------------------------|---------------------|------------------------|--------------------|---------------------|
| Exp. | 0 | 0.0 % | 72.8 | 0 % | 998.8 | 1.003 | 1.002 |
| | 5 % | 1.6 % | 74.4 | 2 % | 1034.0 | 1.002 | 1.036 |
| | 10 % | 3.3 % | 76.2 | 5 % | 1070.6 | 1.013 | 1.085 |
| | 15 % | 5.2 % | 77.9 | 7 % | 1108.5 | 1.215 | 1.347 |
| Ekstr. | 22 % | 8.1 % | 80.5 | 11 % | 1164.0 | 1.440 | 1.676 |

Table 2: Properties for salt water concentration at $T = 20^\circ\text{C}$ from [8]. ρ is interpolated/ extrapolated from data in [9].

The weight percentage is defined as $wt = m_{\text{surfactant}}/m_{\text{total}}$. While 20% addition of salt increases the surface tension by about 10%, density is increased by 16.5% and dynamic viscosity by 43%.

Results

The main data collection in these experiments was images, and in order to get data such as bubble size distribution, bubble speed, and area coverage from these images, automated post processing was the desired path. Unfortunately, automated post processing was not achieved during the project, despite significant efforts in enhancing image quality, lighting etc. In order to obtain quantitative data, a manual analysis was performed on a selected set of experiments, as described in the following section. In addition to the quantitative measurements, a qualitative assessment of the overall behavior under various conditions is given, following the quantitative section.

Quantitative behaviour

The manual analysis is performed on each of the solutions considered at anode inclination of 2 degrees and gas flow rate of 1.5 Slpm (standard liter per minute). Two kinds of measurements were performed, aiming to quantify the collective time evolution of bubbles and typical velocity and size distributions.

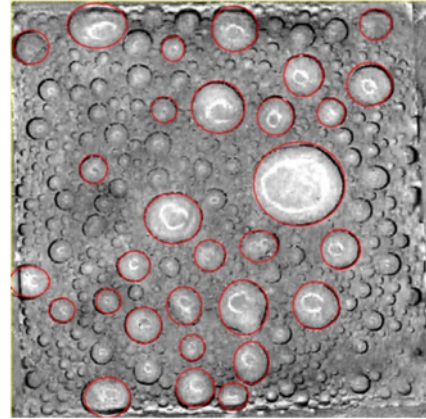


Figure 2: Identification of 30 largest bubbles for ethanol solution.

The time evolution is quantified by tracking the 30 largest observed bubbles over an interval of 8 seconds, with frames separated by 0.16 seconds. Figure 2 shows a typical frame with 30 identified bubbles for the ethanol case.

The collective measurements indicated above yields the time evolution of maximum and minimum bubble area and the coverage fraction, defined as

$$A_{\text{cov}} = \frac{A_b(t)}{A_{\text{anode}}} \quad (1)$$

Where $A_b = \sum_{i=1}^{30} A_{b,i}$ is the sum over the 30 largest bubbles, $A_{b,i}$, in a given frame, and A_{anode} is the anode surface (10 by 10 cm), thus giving an indication of the temporal evolution of the coverage rate of the largest bubbles. The evolution of bubble size and relative coverage is shown in Figure 3-6.

Experiments with the salt solution show the clearest tendency towards self-organization, characterized by a collective motion of large bubbles, resulting in a low frequency, high amplitude variation of the relative coverage, with an estimated period of 2.5 s, equal to 0.4 Hz. The coverage fraction is correlated to the presence of large bubbles indicated in Figure 4. The largest bubbles in the salt solution are approximately 4 times larger than the corresponding bubbles in water, while the bubbles in the ethanol solution are approximately 2 times larger. Figure 5 shows that the minimum bubble area, $\min_i A_{b,i}(t)$, for the three cases are fairly similar, indicating that a sampling of 30 bubbles is sufficient.

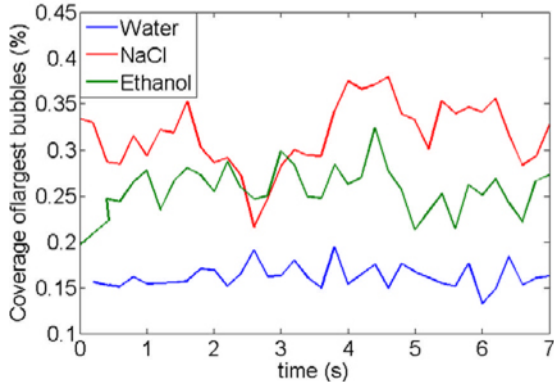


Figure 3: Coverage fraction of the 30 largest bubbles as a function of time.

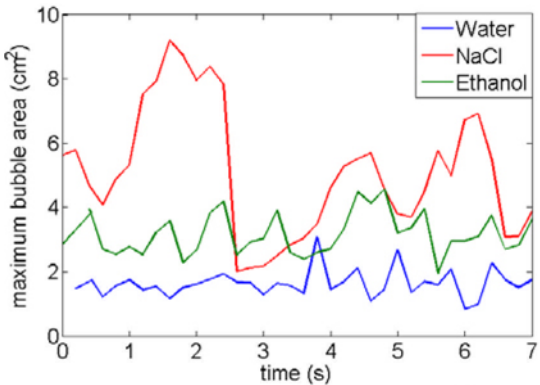


Figure 4: Maximum bubble area, $\max_i A_{b,i}(t)$, as a function of time.

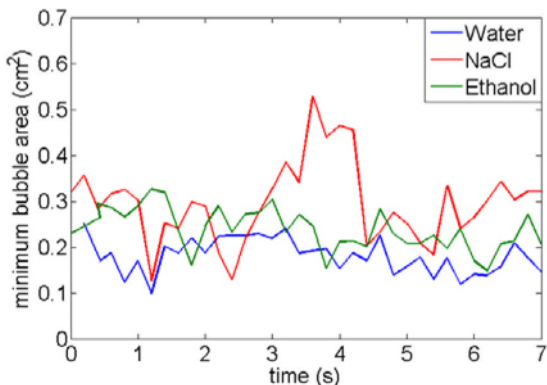


Figure 5: Minimum bubble area, $\min_i A_{b,i}(t)$, as a function of time.

To quantify bubble velocity, 5 bubbles per experimental setup were tracked, separated by 2-8 frames, depending upon how rapidly they moved. Based upon differences in the centroid position and the time between consecutive frames, a (mean) bubble velocity was estimated. Bubbles of different sizes and at different positions were sampled on the porous plate in order to obtain representative values. Figure 6 shows the measured bubble velocities plotted versus bubble area. Two interesting observations can be drawn from the figure:

- We clearly see a distribution of considerably smaller bubbles in water, compared to the other two solutions. It is also, as was indicated in Figure 4, evident that the salt solution has the largest bubbles.
- Although significantly larger bubbles were found in the salt solution, these move, contrary to what is expected due to buoyancy, considerably slower than the small bubbles in the pure tap water.

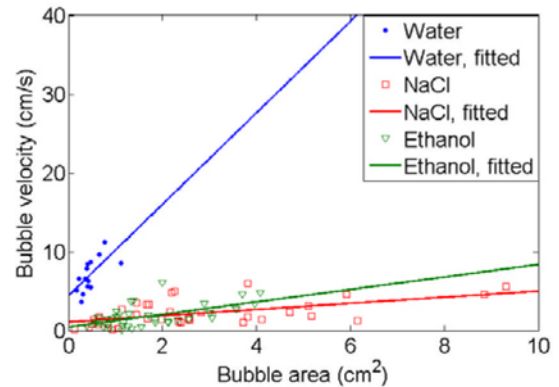


Figure 6: Bubble velocity as a function of bubble area.

Qualitative analysis

The qualitative analysis is based on observations of video footage and rough measurements in order to give an indication of the influence of parameters not considered in the quantitative analysis.

Figure 7 shows instantaneous images with 0.25s intervals of N_2 bubbles in tap water, at 1 degree inclination and 1.5 Slpm flow rate. The bubbles move with a speed of 4-12 cm/s, depending on size and location, across the anode. These speeds indicate semi-rigid type of bubbles in the wetting film regime [10] [11] characterized by an almost circular shape with only weak oscillations. A tiny bubble created close to the left picture rim of the anode spends approximately 2-3s before escaping on the right side. Along the way it coalesces into bubbles and escape on the right picture side with an estimated diameter of 2-3cm. There is a tiny flow in the leftward direction close to "downhill" edge of the anode (indicated in the top left of Figure 7). In correspondence with [12] [13] lower anode inclination appears to promote lower bubble velocities and larger bubble sizes while larger inclination has the opposite effect.

Figure 8 shows 6 frames of a mixture of 15% weight percentage of ethanol. Ethanol has lower surface tension than water, such that the total surface tension for the mixture was calculated as 42mN/m. This is a reduction in surface tension of 40% (Table 2). Visibility is somewhat reduced compared to the tap water experiment making small bubbles more difficult to track. A significant difference between the bubble behavior in the ethanol mixture and the tap water flow is the division of flow into two opposite directions. A great portion of the bubbles travel against buoyancy, whereas in the tap water case almost all bubbles moved with buoyancy (left to right in figure). The split of directions occurs at a line slightly left of the anode horizontal center line (see Figure 8 T=0). The bubbles are slightly elongated parallel to the flow, and the translational behavior is more of the grow-slip type

described as creeping/transitional motion by [10]. Small bubbles move with a speed less than 2 cm/s. At the front edge of the anode the bubble is stretched, and finally the rear end slips. In the tap water case the bubble grows and moves more or less at the same time

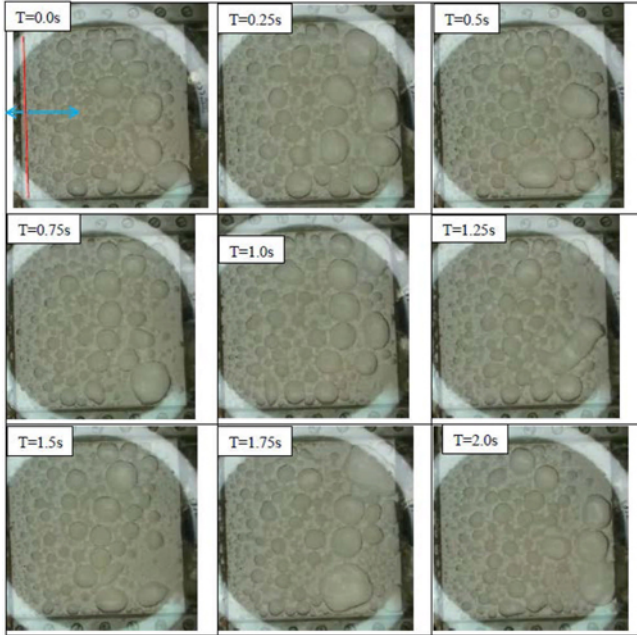


Figure 7: Instantaneous pictures of tap water case for 1degree inclination and flow rate 1.5Slpm at 0.25s intervals.

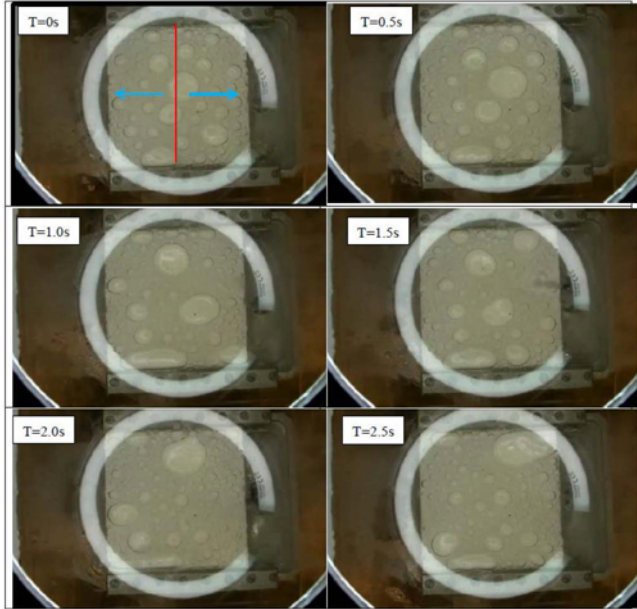


Figure 8: Instantaneous pictures of water-15% ethanol mixture for 1degree inclination and flow rate 1.5Slpm at 0.5s intervals.

Salt has a lower effect on surface tension per weight percentage than ethanol. Since it was desired to change the surface tension of the mixture containing as much as possible, within the solubility

limit of salt in water, a weight percentage of 22% NaCl was used finally in the salt experiment. The surface tension for this mixture was estimated to be 80.5mN/m , which is approximately 10% higher than for tap water. A drawback with this high concentration of salt was that the optical conditions were severely reduced as can be seen from Figure 9. Large bubbles are clearly visible, but smaller bubbles almost disappear. The bubbles in the 22% salt solution behave similar to the bubbles in the ethanol solution. They have a creeping type motion, before they rapidly accelerate in the same manner as in the ethanol mixture. The bubbles escape to both sides as in the ethanol case, but the line dividing the two directions is closer to the "downhill" left edge. The bubbles become larger than in the other two solutions, and in some cases cover a fraction of ~40% of the anode surface. Bubble translational velocity is slightly lower than for the ethanol case, and the bubble shape appears more spherical..

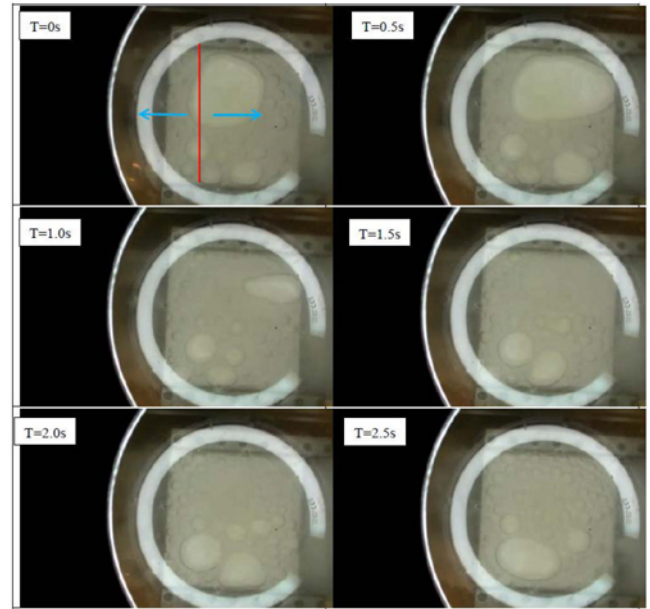


Figure 9: Instantaneous pictures of water-22% Salt mixture for 1degree inclination and flowrate 1.5Slpm at 0.5s intervals.

Discussion

The analysis of the video footage clearly shows that there are significant differences in the bubble behavior under the various conditions considered.

Velocity

An emerging question from the experiments is what causes the large difference in bubble speed between the fluids? As the surface tension has been altered in opposite directions for the ethanol and salt solutions this indicates that surface tension alone cannot explain the observations. Turning to dimensional numbers for an explanation the only number that is purely dependent on mixture properties is the Morton number defined as

$$Mo = \frac{gv_l^4 \rho_l^3}{\sigma^3} \quad (2)$$

Where g is gravity, v_l liquid kinematic viscosity, ρ_l liquid density, and σ is surface tension. For the three solutions, Mo_{water} is an order of magnitude smaller than for the other two solutions (Table

3). Bubbles in low Mo liquids are more deformable than in high Mo liquids, and the terminal speed is found to increase with decreasing Mo [14]. The Bond number defined as

$$Bo = \frac{g\rho_l d_b^2}{\sigma} \quad (3)$$

where d_b^2 is the bubble diameter in mm, is 50% higher in the ethanol solution than for the tap water and salt solution. Terminal speed of bubbles is found to increase with $Bo^{0.7}$ for Mo in the current range [14]. In the case of salt solutions [15] found the terminal speed to be lowered significantly and credited it to the disjoining pressure effect. In the experiments bubbles in the ethanol and salt solutions do not reach their terminal speed before leaving the surface, but its theoretical value still gives an indication of the magnitude of the net force acting on the bubble.

Table 3: Morton and Bond number for the three solutions. d_b is here to be given in mm.

| Solution | Mo | Bo |
|-----------------------|---------|-------------|
| Tap water | 2.6E-11 | $0.14d_b^2$ |
| Tap water-15% Ethanol | 1.4E-10 | $0.22d_b^2$ |
| Tap water-22% NaCl | 1.3E-10 | $0.14d_b^2$ |

Wetting

According to the above findings one could expect bubbles of the same size to travel faster in tap water than in the ethanol and salt solutions, but on the other hand the bubbles in these solutions are considerably larger and should therefore travel faster due to larger buoyancy. The explanation seems to be related to the wetting conditions in terms of the initial start of movement, creeping flow, film generation and maintenance. The starting movement is related to an imbalance of forces between the buoyancy and adhesion as deduced by [16]. The critical adhesion tension, $\Delta\sigma_C$, before a rolling motion started was estimated as

$$\Delta\sigma_C = \sigma[\cos(\theta_{Rc}) - \cos(\theta_{Ac})] \quad (4)$$

θ_{Rc} and θ_{Ac} are the static critical wetting angles of the front and rear parts of the bubble respectively. Since σ of the salt and ethanol solutions vary above and below the value for water it implicates that in order to explain our observations, the difference between θ_{Rc} and θ_{Ac} is larger in these solutions. A wetting experiment was carried out to quantify θ_{Rc} and θ_{Ac} [17], but the results gave no indication of a larger contact angle hysteresis. The measurements are however not fully finalized. At the critical angles an internal motion of the bubble is initiated where gas is torn from the rear and moved to the front [16] and starts a creeping motion characterized by [10] as a battle between dynamic wetting and dewetting. This creeping motion persists until a perturbation in the front lifts the bubble and initiates the film generation process [10]. In our case the transitions in the salt and ethanol solutions are static, or creeping, until the bubble becomes considerably larger than in the water case that has an early transition. The exact relation to wetting is however not determined.

Coalescence

Another puzzling question is the difference in the evolution of bubble size. It is clear that the ethanol and salt solutions promote larger bubbles than that obtained in tap water. This is somewhat in contradiction from what could be expected when considering the effects of both these type additives reported in coalescence studies [18] [19]. In both these studies, although the compounds were slightly different from what was used in this work, the effect of salt and alcohol was to increase coalescence time. The factor that evidently makes up for the assumed poorer coalescence properties must be the collision frequency and speed or surface polarization effects. In the tap water the bubbles moved more uniformly giving less frequent collisions, while in the other two mixtures the grow-slip type behavior leads to frequent impact. Also, the larger speed of the water bubbles leads to less time for coalescence before reaching the anode surface edge. An artifact is that small bubbles in purified water have been found to be quite stable [19], but that small natural impurities usually found in tap water removes this stability. Whether the purity of the water plays a role in its lower coalescence rate in the current case is not known.

Fluid flow

The splitting of the flow into two directions and the difference between the three solutions is a new phenomenon observed during this investigation. A rigid explanation cannot be given here since flow measurements in the liquid were not performed. However it seems plausible that it is strongly linked to bubble velocity. For a flat anode, Figure 10 a), it is observed that the splitting line is at the anode center. This gives the shortest escape path for each bubble, and the drag from the bubbles generates and maintains two similar vortices systems. The loss in the system is mainly caused by the friction of the flow towards the walls. In the inclined case, Figure 10b), the buoyancy would generate a stronger bubble drift towards the "uphill" right side and increase the vortex system at this side. From the experiments it appears that when the drag from the bubbles is large, as in the tap water case, a large vortex is formed covering almost the whole anode. For the other two cases the energy supplied from the bubbles is insufficient to accelerate one large vortex.

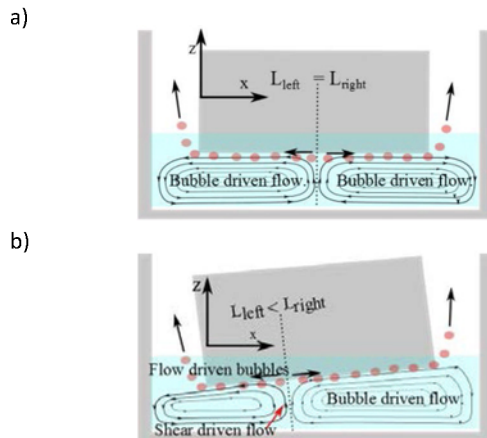


Figure 10: Illustration of a simplified flow pattern under anode for flat and inclined case.

It requires less energy to split the flow at a downhill position and maintain this smaller vortex at this side in addition to accepting the negative work from the bubbles. The negative work from the bubbles will also lower the velocity of the vortex on this side, and

consequently also lower the frictional losses. The further downhill shift of the salt solution compared to the ethanol solution, despite equal or lower velocities, could be related to the higher viscosity of the salt solution. Bubbles in the salt solution would induce a larger drag force.

Conclusion

Experiments on a lab scale water model have been performed in order to identify the influence of various parameters on bubble flow. Surface tension has been given particular attention and has been reduced using ethanol and increased by adding NaCl. Significant changes in flow regime were observed for the different solution. Kinematic viscosity did not vary significantly from the tap water for the ethanol solutions, while for the salt solution there was a considerably increase. The following conclusions can be drawn from the study:

- 1) Bubbles in the NaCl solutions are the largest.
- 2) Bubbles in the NaCl solution, despite larger volumes, travel at significantly lower velocities than that observed in tap water.
- 3) Only the NaCl solution appears to be close to a self-organized state.
- 4) Bubbles in the ethanol solution tend to be elongated than bubbles in the water and salt solutions
- 5) Ethanol and NaCl solutions enable bubble detachment at both anode edges, despite significant anode inclination.
- 6) Bubbles in ethanol and NaCl solutions show a distinct growth-slip type of behaviour, while bubbles in the water solution show a regular sliding motion on the anode surface.

The data obtained in this study can in principle be used to validate a numerical model and at the same time it indicates the potential challenges in reproducing experimental data where *all* conditions are not known. In this context, the current experiments in combination with simulations can serve as a basis for identifying which parameters which need to be measured in greater detail.

ACKNOWLEDGMENTS

The present work was supported by the project "Gas and Alumina Distribution and Transport" (GADT), financed by the Research Council of Norway and Hydro Primary Metal Technology. Permission to publish the results is gratefully acknowledged.

Bibliography

- [1] R. E. J. Shekhar, "Physical Modeling Studies of Electrolyte Flow Due to Gas Evolution and Some Aspects of Bubble Behavior in Advanced Hall Cells: Part I. Flow in Cells with a Flat Anode," *Metallurgical and Materials Transactions B*, vol. 25B, no. June, pp. 333-340, 1994.
- [2] Y. Feiya, M. Dupuis, Z. Jianfei and R. Shaoyong, "In Depth Analysis Of Energy Saving And Current Efficiency Improvement Of Aluminum Reduction Cells," *Light Metals*, pp. 537-542, 2013.
- [3] M. Alam, Y. Morsi, G. Mohanarangam and J. Chen, "Investigation of electrolytic bubble behaviour in aluminum smelting cell," *Light Metals*, pp. 591-596, 2013.
- [4] I. Eick, A. Klaveness, K. Rosenkilde, M. Segatz, H. Gudbrandsen, A. Solheim, E. Skybakmoen and K. E. Einarsrud, "Voltage and Bubble release behaviour in a laboratory cell at low anode-cathode distance," in *10th AASTC*, Launceston, Australia, 2011.
- [5] K. Einarsrud, S. Johansen and I. Eick, "Anodic bubble behaviour in Hall-Heroult Cells," in *TMS 2012*, 2012.
- [6] R. E. Maples, *Petroleum Refinery Process Economics* (2nd ed.), Pennwell Books, 2000.
- [7] G. Vazquez, E. Alvarez and J. Navaza, "Surface Tension of Alcohol + Water from 20 to 50C," *J. Chem. Eng. Data*, no. 40, p. 611 – 614, 1995.
- [8] A. Horibe, S. Fukusako and M. Yamada, "Surface tension of low-temperature aqueous solution," *International Journal of Thermophysics*, vol. vol 17, no. 2, pp. 483- 493, 1996.
- [9] D. Lide, *CRC handbook of chemistry and physics*, 86 ed., Boca Raton, 2005.
- [10] A. Perron, L. Kiss and S. Poncsák, "An experimental investigation of the motion of single bubbles under a slightly inclined surface," *International Journal of Multiphase Flow*, vol. 32, pp. 606-622, 2006.
- [11] A. Perron, L. I. Kiss and S. Poncsák, "Regimes Of The Movement Of Bubbles Under The Anode In An Aluminum Electrolysis Cell," *Light Metals*, pp. 565-571, 2005.
- [12] S. Poncsák, L. Kiss, T. Dominic, A. Perron and S. Perron, "Size Distribution Of The Bubbles In The Hall-Héroult Cells," *Light Metals*, pp. 457-462, 2006.
- [13] S. Fortin, A. Gerhardt and A. Gesing, "Physical modeling of bubble behavior and gas release from aluminum reduction cell anodes," *Light Metals*, pp. 721-741, 1984.
- [14] A. Perron, L. Kiss and S. Poncsák, "Motion of singles bubbles moving under a slightly inclined surface through stationary liquids," *International Journal of Multiphase Flow*, vol. 32, pp. 1311-1325, 2006.
- [15] L. Castillo, O. Satomi, L. White, S. Carnie and R. Horn, "Effect of disjoining pressure on terminal velocity of a bubble sliding along an inclined wall," *Journal of Colloid and Interface Science*, vol. 364, pp. 505-511, 2011.
- [16] Y. Frenkel, "On the behavior of liquid drops on a solid surface: 1. The sliding of drops on an inclined surface," *J.Exptl. Theoret. Physics*, vol. 18, p. 659, 1948.
- [17] A. Solheim, H. Gulbrandsen, A. Martinez, K. Einarsrud and I. Eick, "Wetting Between Carbon And Cryolitic Melts., Part II: Effect of bath properties and polarisation" *Light Metals*, 2015.
- [18] L. Castillo, S. Ohnishi and R. Horn, "Inhibition of bubble coalescence: Effects of salt concentration and speed of approach," *Journal of Colloid and Interface Science*, vol. 356, pp. 316-324, 2011.
- [19] S. Samanta and P. Ghosh, "Coalescence of air bubbles in aqueous solutions of alcohols and nonionic surfactants," *Chemical Engineering Science*, vol. 66, pp. 4824-4837, 2011.
- [20] W. Zhang, J. Chen and M. Taylor, "Similarity Analysis Of Gas Induced Bath Flow In Hall-Heroult Cells," in *18'th Australasian Chemical Engineering Conference*, Auckland, New Zealand, 1990.